© 2016. Published by The Company of Biologists Ltd | Disease Models & Mechanisms (2016) 9, 1211-1220 doi:10.1242/dmm.025536

RESEARCH ARTICLE

SPECIAL COLLECTION: TRANSLATIONAL IMPACT OF RAT

Identification of gene expression patterns crucially involved in experimental autoimmune encephalomyelitis and multiple sclerosis

Martin M. Herrmann[1], Silvia Barth[1], Bernhard Greve[1], Kathrin M. Schumann[1], Andrea Bartels[1] and Robert Weissert[1,2,*]

ABSTRACT

After encounter with a central nervous system (CNS)-derived autoantigen, lymphocytes leave the lymph nodes and enter the CNS. This event leads only rarely to subsequent tissue damage. Genes relevant to CNS pathology after cell infiltration are largely undefined. Myelin-oligodendrocyte-glycoprotein (MOG)-induced experimental autoimmune encephalomyelitis (EAE) is an animal model of multiple sclerosis (MS), a chronic autoimmune disease of the CNS that results in disability. To assess genes that are involved in encephalitogenicity and subsequent tissue damage mediated by CNS-infiltrating cells, we performed a DNA microarray analysis from cells derived from lymph nodes and eluted from CNS in LEW.1AV1 (*RT1*^{av1}) rats immunized with MOG 91-108. The data was compared to immunizations with adjuvant alone or naive rats and to immunizations with the immunogenic but not encephalitogenic MOG 73-90 peptide. Here, we show involvement of *Cd38*, *Cxcr4* and *Akt* and confirm these findings by the use of *Cd38*-knockout (B6.129P2-*Cd38*^{tm1Lnd}/J) mice, S1P-receptor modulation during EAE and quantitative expression analysis in individuals with MS. The hereby-defined underlying pathways indicate cellular activation and migration pathways mediated by G-protein-coupled receptors as crucial events in CNS tissue damage. These pathways can be further explored for novel therapeutic interventions.

KEY WORDS: Experimental autoimmune encephalomyelitis, Multiple sclerosis, Central nervous system, Cellular traffic, T cell, Adjuvant

INTRODUCTION

Multiple sclerosis (MS) is a disease of the central nervous system (CNS) that leads to chronic inflammation, demyelination, and axonal and neuronal loss, resulting in disability (Noseworthy et al., 2000; Weissert, 2013). Myelin-oligodendrocyte-glycoprotein (MOG)-induced experimental autoimmune encephalomyelitis (EAE) in rats reproduces major aspects of the human pathology (Weissert et al., 1998b; Storch et al., 1998; Kornek et al., 2000; Weissert, 2016). MOG is expressed on the outer surface of the myelin sheath. In contrast to merely T-cell-mediated animal models, the pathogenesis of MOG-induced EAE in the rat involves the combined action of T and B cells, antibodies and macrophages, mimicking type II lesions in MS (Genain et al., 1995; Mathey et al., 2004; Lucchinetti et al., 2000).

Encephalitogenic peptides presented on MHC class II molecules to T cells lead to a program that forces lymphocytes to be activated and migrate towards the CNS (Riedhammer and Weissert, 2015). Adjuvant contributes by affecting multiple signaling pathways in lymphocytes as well as in organ-resident cells like in the CNS. We have previously demonstrated that MOG 91-108 is the major determinant to trigger disease in rats expressing *RT1*^{av1} or *RT1*^{n} haplotypes (Weissert et al., 2001). Interestingly, the capacity of MOG 91-108 to induce EAE was dissociated in regard to Th1 or Th2 cytokine expression in lymphoid tissue compared to the CNS. Moreover, different MOG 1-125-derived peptides, such as MOG 73-90, were immunogenic, showing strong Th1 responses, but were not encephalitogenic. The induction of active EAE in LEW MHC congenic rat strains and Dark Agouti (DA) (*RT1*^{av1}) rats does not require the application of pertussis toxin like in mice. This is an advantage because the exact role of pertussis toxin in EAE induction is not clear so far. Pertussis toxin inhibits Gi proteins and thereby influences multiple cellular processes and pathways (Dumas et al., 2014). Active EAE in susceptible rat strains is induced by immunization with an encephalitogenic peptide mixed with mineral oil [incomplete Freund's adjuvant (IFA)] with the addition of heat-inactivated mycobacterium tuberculosis (MT) as adjuvant [complete Freund's adjuvant (CFA)]. MT leads by binding and signaling through Toll-like receptors (TLRs) to an activation program in a number of cell types and is also a systemic 'danger signal' (Mills, 2011).

In regard to susceptibility to EAE and MS, gene expression profiling studies have been performed to elucidate genes that are involved in disease pathogenesis. A number of interesting genes were described, such as osteopontin (Hur et al., 2007). In no study was a systematic comparison of gene expression profiles performed in EAE in which the influence of adjuvant and antigen was systematically compared on the expression profile of lymph node (LN)-derived cells or cells eluted from CNS of diseased animals. In the present study, we systematically compared the gene expression profiles of cells from draining LNs and CNS-infiltrating cells that were eluted in LEW.1AV1 (*RT1*^{av1}) rats immunized with MOG 91-108 in CFA, CFA alone and in naive rats. Moreover, we compared the gene expression profile of rats immunized with the encephalitogenic MOG peptide 91-108 with rats immunized with the non-encephalitogenic MOG peptide 73-90. We found differentially expressed genes that are of major importance for

[1]Department of General Neurology, Hertie Institute for Clinical Brain Research, University of Tübingen, 72076 Tübingen, Germany. [2]Department of Neurology, University of Regensburg, 93053 Regensburg, Germany.

*Author for correspondence (robert.weissert@ukr.de)

R.W., 0000-0002-1295-1271

Received 29 March 2016; Accepted 9 August 2016

Disease Models & Mechanisms (2016) 9, 1211-1220 doi:10.1242/dmm.025536

encephalitogenicity. The influence of these genes was subsequently verified by different means.

RESULTS

Gene expression after immunization with encephalitogenic and non-encephalitogenic peptides

One of the important issues in MS and other inflammatory diseases of the CNS is understanding the requisites of autoantigenic peptides to induce CNS inflammation (Riedhammer and Weissert, 2015). Beside presentation of autoantigen-derived peptides on MHC molecules and the availability of reactive T-cell and B-cell repertoires as well as the presence of the target antigen in the CNS, pathways of cellular activation exist that allow disease development. These pathways are presently only partly elucidated. We used MOG-induced EAE in LEW.1AV1 ($RT1^{av1}$) rats as a model system for CNS inflammation. In this EAE model, the determinant MOG 91-108 is immunogenic and encephalitogenic. In contrast, the determinant MOG 73-90 is immunogenic but not encephalitogenic. We assessed the gene expression profiles by gene arrays of lymphocytes from draining LNs and from lymphocytes eluted from the CNS.

To focus on genes that are truly relevant to encephalitogenicity and not simply involved in general inflammatory responses, we compared gene arrays of LEW.1AV1 ($RT1^{av1}$) rats immunized with the encephalitogenic MOG stretch MOG 91-108 to naive LEW.1AV1 ($RT1^{av1}$) rats and rats immunized with the adjuvant CFA alone as well as rats immunized with the non-encephalitogenic MOG 73-90 determinant. We analyzed ten comparisons for each of the naive and CFA groups versus MOG 91-108 and five comparisons for MOG 73-90 versus MOG 91-108. The number of comparisons in which a given gene had a signal log ratio (SLR) of above 1 was counted. In Table 1, we show genes that are upregulated in at least half of the comparisons (=50%). Besides *Cxcr4* and *Cd38*, which were subsequently analyzed in greater detail, many genes with a known function in EAE and MS pathology were found to have an increased expression in MOG 91-108-immunized rats as compared to controls. This validates our gene list and supports the relevance of the genes not previously described in EAE. In Table S1, genes with decreased expression in EAE are listed. In this analysis, the variability between gene arrays was much higher and fewer genes were found to be regulated with a clear pattern according to our criteria.

Comparisons of microarrays of CNS-infiltrating lymphocytes derived from LEW.1AV1 ($RT1^{av1}$) rats after immunization with MOG 91-108, MOG 73-90 and CFA alone resulted in many more genes being differentially expressed as compared to the analysis of LN cells (Tables S2 and S3). This could mirror the influx of different cell populations into the CNS during an inflammatory attack. Similar to the analysis of LN cells, we found that *Cd38* and *Cxcr4* mRNA was strongly increased in CNS-infiltrating cells.

Subsequently, we analyzed purified $CD4^+$ cells from LNs and CNS of MOG 91-108- and MOG 73-90-immunized rats. To some extent, similar gene expression profiles were found in the purified $CD4^+$ cell population compared to non-separated LN cells (Table 1, Tables S4 and S5).

Owing to their strong expression in MOG 91-108-immunized rats compared to naive, CFA-immunized and MOG 73-90-immunized rats, we chose *Cxcr4* and *Cd38* for further analysis.

Cxcr4 and *Cd38* in EAE in LEW.1AV1 ($RT1^{av1}$) rats

Confirming our microarray results by quantitative PCR, we found a significant upregulation of *Cxcr4* expression in LN cells of MOG 91-108-immunized rats (n=8) as compared to CFA-immunized (n=8, ANOVA, P<0.0001) and naive (n=6, ANOVA, P<0.0001) LEW.1AV1 ($RT1^{av1}$) rats (Fig. 1A). Also, an increased expression of *Cd38* was measured [MOG 91-108-immunized rats (n=8) as compared to CFA-immunized (n=8, ANOVA, P<0.05) and naive (n=6, ANOVA, P<0.05) LEW.1AV1 ($RT1^{av1}$) rats].

In cells eluted from the CNS, we found upregulation of *Cxcr4* (Fig. 1B) and *Cd38* (Fig. 1C) in MOG 91-108-immunized LEW.1AV1 ($RT1^{av1}$) rats (n=6) compared to rats immunized with MOG 73-90 (n=6, ANOVA, *Cxcr4* and *Cd38* each P<0.001) or CFA alone (n=6, ANOVA, *Cxcr4* and *Cd38* each P<0.001).

Cxcr4 and *Cxcl12* expression in spinal cord of DA ($RT1^{av1}$) rats

Next, we assessed the mRNA expression of *Cxcr4* (Fig. 2A) and its ligand *Cxcl12* (Fig. 2B) in spinal cord of either naive DA ($RT1^{av1}$) rats or DA ($RT1^{av1}$) rats immunized with IFA or CFA alone or MOG 1-125 in IFA or MOG 1-125 in CFA (each n=4). Upregulation of both *Cxcl12* and *Cxcr4* mRNA expression was observed in CFA- and MOG 1-125 in CFA-immunized DA ($RT1^{av1}$) rats in spinal cord compared to naive rats, IFA-injected or MOG 1-125 in IFA-immunized DA ($RT1^{av1}$) rats (ANOVA, P<0.001). Increased *Cxcl12* and *Cxcr4* mRNA expression was observed in MOG 1-125 in CFA- compared to CFA-immunized DA ($RT1^{av1}$) rats (ANOVA, P<0.01).

Cxcr4 and CXCL12 in individuals with MS

Upregulation of *CXCR4* mRNA was also observed in white blood cells of individuals with MS with a relapsing-remitting disease course (RRMS; n=32) and a secondary chronic progressive disease course (SPMS; n=22), and compared to controls (n=25, ANOVA, RRMS and SPMS each P<0.05) (Fig. 3A, Tables S6 and S7). Also, we detected increased protein CXCL12 serum levels in both individuals with RRMS (n=24) and SPMS (n=28) compared to controls (n=21, ANOVA, RRMS and SPMS each P<0.05) (Fig. 3B, Tables S6 and S7).

EAE in B6.129P2-*Cd38*^{tm1Lnd}/J mice

Cd38 was strongly upregulated in encephalitogenic LN cells. To functionally validate our data and to elucidate the role of CD38 in EAE, we induced disease with the extracellular domain of MOG (MOG 1-125) in *Cd38*-knockout (B6.129P2-*Cd38*^{tm1Lnd}/J) mice and appropriate controls. We found reduced disease severity in MOG 1-125-immunized B6.129P2-*Cd38*^{tm1Lnd}/J mice (n=22) compared to wild-type control mice (n=21, t-test, cumulative disease score P<0.01) (Fig. 4A). Next, we determined the height of the antibody response to MOG 1-125. Reduced anti-MOG IgG autoantibody responses in B6.129P2-*Cd38*^{tm1Lnd}/J mice (n=4) compared to wild-type control mice (n=4, ANOVA, P<0.05) after immunization with MOG 1-125 were seen (Fig. 4B) on day 12 post-immunization (p.i.). Furthermore, also T-cell responses upon restimulation with MOG 1-125 were reduced in the B6.129P2-*Cd38*^{tm1Lnd}/J mice (n=4) on day 12 p.i. compared to control mice (n=4, t-test for stimulation with 50 µg/ml MOG 1-125, P<0.05) as measured in a proliferation assay, indicating in addition a T-cell priming or expansion defect in B6.129P2-*Cd38*^{tm1Lnd}/J mice (Fig. 4C).

Targeting cellular migration by FTY720

We found an upregulation of *Akt* in our differential gene expression studies (Table 1). FTY720 is an S1P-receptor modulator known to influence T-cell trafficking by an *Akt*-dependent mechanism, as

Table 1. Genes with increased expression in lymph-node cells of LEW.1AV1 (*RT1*^{av1}) rats

Gene symbol	Gene name	Affymetrix probe set ID	MOG 91-108 vs naive percentage	MOG 91-108 vs naive average SLR	MOG 91-108 vs CFA percentage	MOG 91-108 vs CFA average SLR	MOG 91-108 vs MOG 73-90 percentage	MOG 91-108 vs MOG73-90 average SLR	Function (putative)
Hmgcs2	3-hydroxy-3-methylglutaryl-CoA synthase 2	M33648_g_at	100	3.27	100	1.39	100	2.15	Metabolism
Ptpn16	Protein tyrosine phosphatase non-r. type 16	U02553cds_s_at	100	3.22	80	1.87	100	3.00	Intracellular signaling
Cxcr4	Chemokine receptor (LCR1)	rc_AA945737_at	100	1.94	80	1.48	100	1.67	Chemokine receptor
Ccl3	Chemokine (C-C motif) ligand 3	U22414_at	90	2.68	70	1.86	60	0.72	Chemokine
Jun	v-jun sarcoma virus 17 oncogene homolog	rc_AI175959_at	80	2.19	100	2.95	60	1.12	Intracellular signaling
Cd38	CD38 antigen	rc_AA819187_s_at	60	1.75	100	2.62	60	0.98	Ectoenzyme cADPR
Max	Max	D14447_at	50	2.79	60	2.96	100	2.21	Cell cycle
Cxcl2	Chemokine (C-X-C motif) ligand 2	U45965_at	100	6.63	80	2.21			Chemokine
Il1b	Interleukin 1 beta	E01884cds_s_at	100	4.64	60	1.32			Chemokine
Cebpb	CCAAT/enhancer binding protein (C/EBP), beta	S77528cds_s_at	100	4.55	80	2.68			Cell cycle
Ass	Arginosuccinate synthetase	X12459_at	100	4.55	60	1.77			Metabolism
Arg1	Arginase 1	J02720_at	100	4.36	50	1.43			Metabolism
Fcgr3	Fc receptor, IgG, low affinity III	M32062_g_at	100	4.26	80	1.86			Complement receptor
Ptgs2	Prostaglandin-endoperoxide synthase 2	S67722_s_at	100	3.95	60	1.96			Inflammation
Spp1	Secreted phosphoprotein 1	M14656_at	100	3.49	50	1.13			Inflammation
Olr1	Oxidised low density lipoprotein receptor 1	rc_AI071531_s_at	100	3.37	80	2.04			Metabolism
Nos2	Nitric oxide synthase 2, inducible	U03699complete_seq_at	100	3.19	80	2.71			Inflammation
Anpep	Alanyl (membrane) aminopeptidase	M25073_at	100	3.04	50	1.80			Metabolism
Vegf	Vascular endothelial growth factor	rc_AA850734_at	100	2.81	50	1.28			Growth factor
Igsf6	Immunoglobulin superfamily, member 6	AJ223184_at	100	2.73	50	0.85			Unknown
F3	Coagulation factor 3	U07619_at	100	2.32	70	1.54			Coagulation
Edn1	Endothelin 1	M64711_at	90	1.85	50	1.06			Homeostasis
Wap	Whey acidic protein	J00801_at	60	1.27	90	1.65			Milk protein
Junb	Jun-B oncogene	X54686cds_at	60	1.24	50	0.94			Transcription

Continued

Disease Models & Mechanisms (2016) 9, 1211-1220 doi:10.1242/dmm.025536

Table 1. Continued

Gene symbol	Gene name	Affymetrix probe set ID	MOG 91-108 vs naive percentage	MOG 91-108 vs naive average SLR	MOG 91-108 vs CFA percentage	MOG 91-108 vs CFA average SLR	MOG 91-108 vs MOG 73-90 percentage	MOG 91-108 vs MOG73-90 average SLR	Function (putative)
Anp32a	Acidic nuclear phosphoprotein 32 family A	D32209_at	50	0.84	50	1.11			Unknown
LOC286890	Tropomyosin isoform 6	rc_AA866465_s_at	50	2.02	50		100	3.24	Cell structure
Cdkn1b	Cyclin-dependent kinase inhibitor 1B	D83792_at					100	3.20	Cell cycle
Hmgb1	High mobility group box 1	rc_AA944177_at					80	1.12	Transcription
Smstr28	Somatostatin receptor 28	X63574_at					60	1.04	Metabolism
Klf9	Kruppel-like factor 9	D12769_at					60	1.01	Transcription
Cited2	Cbp/p300-interacting transactivator 2	rc_AA900476_at			90	1.84			Transcription
Akt2	Murine thymoma (v-akt) oncogene homolog 2	rc_AI105076_s_at			80	1.64			Intracellular signaling
Hba1	Hemoglobin, alpha 1	X56325mRNA_s_at			60	1.27			Metabolism
Zfp36	Zinc finger protein 36	X63369cds_at			60	0.93			Cell cycle
Sv2b	Synaptic vesicle glycoprotein 2 b	L10362_at			50	1.39			Metabolism
Mmp12	Matrix metalloproteinase 12	X98517_at			50	1.16			Proteases
Hmox1	Heme oxygenase 1	J02722cds_at			50	1.13			Unknown
Klf4	Kruppel-like factor 4 (gut)	L26292_g_at			50	1.05			Transcription
Il1a	Interleukin 1 alpha	D00403_g_at			50	0.99			Chemokine
Slc2a1	Solute carrier family 2, member 1	M13979_at			50	0.87			Metabolism
Dcn	Decorin	Z12298cds_s_at			50	0.85			Extracellular matrix
Gadd45a	Growth arrest and DNA-damage-induced 45a	rc_AI070295_g_at			50	0.75			Cell cycle

LEW.1AV1 (*RT1*^{av1}) rats were immunized with MOG 91-108 in CFA, MOG 73-90 in CFA and CFA alone. Gene expression in lymph node (LN) cells was analyzed using Affymetrix gene arrays. Gene arrays from rats immunized with MOG 91-108 in CFA (pooled samples of at least *n*=3 rats, *n*=5 gene chips) were compared to gene arrays from naive rats (pooled samples, *n*=2 chips), CFA-immunized rats (pooled samples, *n*=2 chips) and MOG 73-90 in CFA-immunized rats (pooled samples, *n*=1 chip) resulting in each ten comparisons for CFA-immunized and naive to MOG 91-108-immunized rats and five for MOG 73-90- to MOG 91-108-immunized rats. The number of comparisons in which a given gene had a signal log ratio (SLR) above 1 were counted. If a gene had an SLR above 1 in 50% of the comparisons it was included in the analysis. ESTs and sequences not corresponding to a gene and duplicates were removed from the table. Genes which fulfilled the criteria in all of the three comparisons are displayed in the shaded part of the table. Genes which fulfilled the criteria only in naive versus MOG 91-108 in CFA comparisons are not displayed here. LN cells were prepared as described (Weissert et al., 2001). cADPR, cyclic adenine nucleotide ribose.

Disease Models & Mechanisms (2016) 9, 1211-1220 doi:10.1242/dmm.025536

Disease Models & Mechanisms (2016) 9, 1211-1220 doi:10.1242/dmm.025536

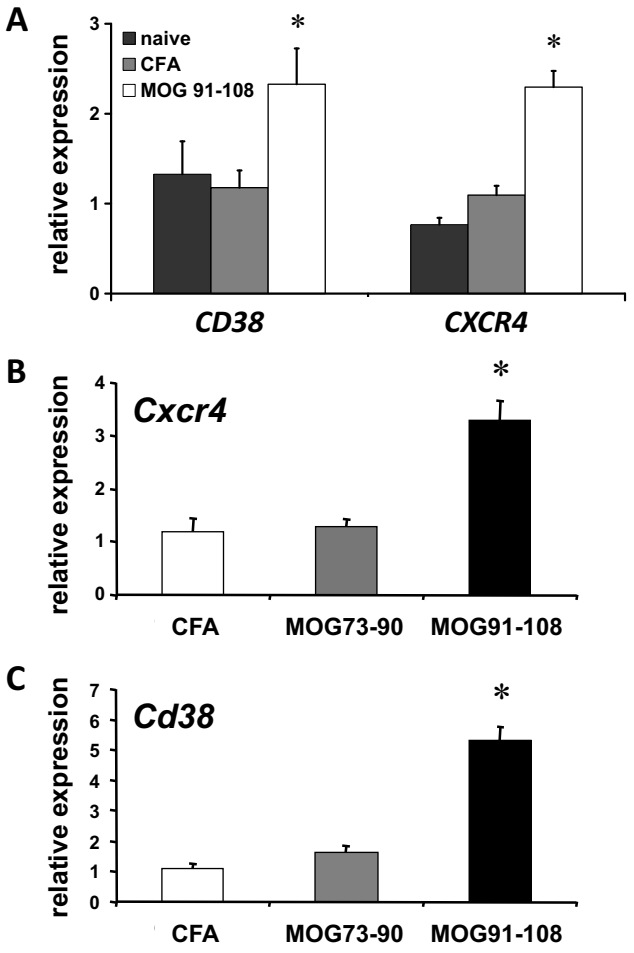

Fig. 1. *Cxcr4* and *Cd38* expression in lymph node cells and CNS. (A) Quantitative SYBR green real-time PCR was performed for *Cxcr4* and *Cd38* in lymph node (LN) cells from naive LEW.1AV1 ($RT1^{av1}$) rats (black bars, n=6), or those immunized with CFA (gray bars, n=8) or MOG 91-108 in CFA (white bars, n=8), on day 12 p.i. Increased *Cxcr4* (ANOVA, *P<0.0001) and *Cd38* (ANOVA, *P<0.05) expression was found in MOG 91-108 in CFA-immunized rats compared to naive and CFA-alone-immunized rats. (B) Quantitative expression of *Cxcr4* in cells eluted from the CNS of CFA (white bars, n=6)-, MOG 73-90 in CFA (gray bars, n=6)- and MOG 91-108 in CFA (n=6)-immunized LEW.1AV1 ($RT1^{av1}$) rats. *Cxcr4* was upregulated in MOG 91-108 in CFA-immunized rats compared to the other groups (ANOVA, *P<0.001) on day 12 p.i. (C) Quantitative expression of *Cd38* of lymphocytes eluted from the CNS of CFA (white bars, n=6)-, MOG 73-90 in CFA (gray bars, n=6)- and MOG 91-108 in CFA (n=6)-immunized LEW.1AV1 ($RT1^{av1}$) rats on day 12 p.i. *Cd38* was upregulated in MOG 91-108 in CFA-immunized rats compared to the other groups (ANOVA, *P<0.001). Results are expressed as $2^{-\Delta\Delta\ CT}$ values. Numbers are mean±s.e.m.

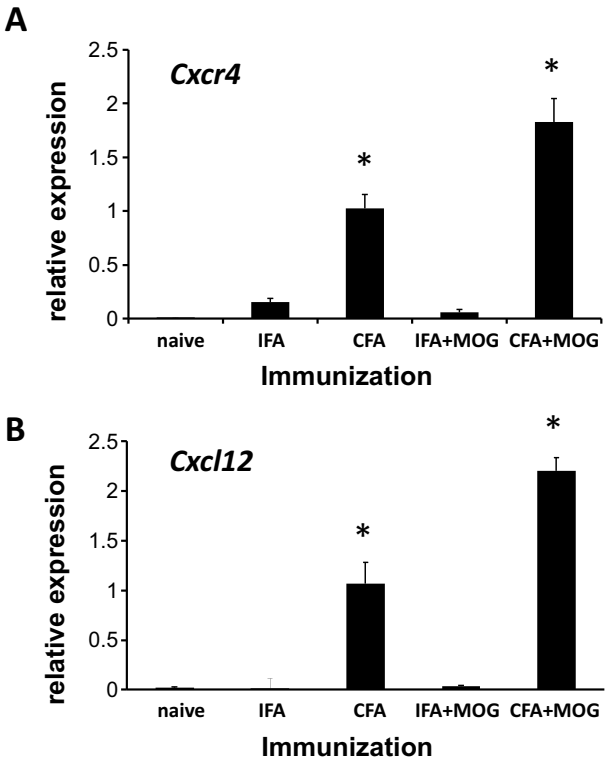

Fig. 2. *Cxr4* and *Cxcl12* expression in spinal cord of DA ($RT1^{av1}$) rats. Quantitative SYBR green real-time PCR was performed for *Cxcr4* (A) and *Cxcl12* (B) from PBS-perfused spinal cord tissue of naive DA ($RT1^{av1}$) rats (n=4), rats immunized with IFA (n=4) or CFA alone (n=4) and DA rats immunized with MOG 1-125 in IFA (n=4) or MOG 1-125 in CFA (n=4) on day 12 p.i. Increased *Cxcr4* and *Cxcl12* expression was observed in spinal cord of DA ($RT1^{av1}$) rats immunized with CFA and MOG 1-125 in CFA (ANOVA, *P<0.001). There was an upregulation of *Cxcr4* and *Cxcl12* mRNA in DA ($RT1^{av1}$) rats immunized with MOG 1-125 in CFA compared to DA ($RT1^{av1}$) rats immunized with CFA alone (ANOVA, *P<0.01). Quantitative PCR results are expressed as $2^{-\Delta\Delta CT}$ values. Numbers are mean±s.e.m.

does CXCR4 (Mandala et al., 2002; Cyster, 2005; Lee et al., 2001; Brinkmann et al., 2002; Matloubian et al., 2004). We evaluated inhibition of *Akt*-dependent cell trafficking in MOG 91-108-immunized LEW.1AV1 ($RT1^{av1}$) rats. Disease was completely inhibited in rats treated from day 0 p.i. with FTY720 (n=10) as compared to the vehicle-treated controls (n=10, t-test, cumulative disease score P<0.0001) (Fig. 5A). Next, we tested the efficacy of FTY720 to treat established relapsing-remitting MOG 1-125-induced EAE in the DA ($RT1^{av1}$) rat. FTY720 treatment was started on day 21 p.i., after the first bout of disease (n=8), and showed a significant effect on the disease course as compared to vehicle treatment (n=8, t-test, cumulative disease score day 21-44 p.i., P<0.01) (Fig. 5B). To further examine the beneficial effect of FTY720 treatment on EAE, we boosted the rats with MOG 1-125 on day 44 after the first immunization. Although a relapse was induced in both groups, the DA rats under FTY720 treatment had a better clinical outcome compared to the vehicle-treated animals (t-test, cumulative disease score day 45-56 p.i., P<0.0001). On day 14 p.i., FTY720 treatment led to an increase of the relative size of the CD4 T-cell compartment (ANOVA, P<0.01) in the treated LEW.1AV1 ($RT1^{av1}$) rats (n=10) compared to controls (n=9) concurrent with a decrease in the CD8 T-cell (ANOVA, P<0.01) and the B-cell (ANOVA, P<0.01) compartment (Fig. 5C; Fig. S1). FTY720 treatment (n=9) compared to controls (n=9) led to the downregulation of mRNA expression of its receptor, *S1p1* (ANOVA, P<0.0001), and of *Akt2* (ANOVA, P<0.0001), one of the genes involved in the intracellular signaling cascade connected to S1P1 and CXCR4, on day 14 p.i. Treatment also had a negative effect on the expression levels of *Cd38* (ANOVA, P<0.0001). In contrast, the expression of *Cxcr4* was not altered (ANOVA, not significant) (Fig. 5D).

DISCUSSION

In this study we identified gene networks that are crucially involved not only in raising an autoantigen-specific immune response but also in constituting encephalitogenicity. We analyzed the

Disease Models & Mechanisms (2016) 9, 1211-1220 doi:10.1242/dmm.025536

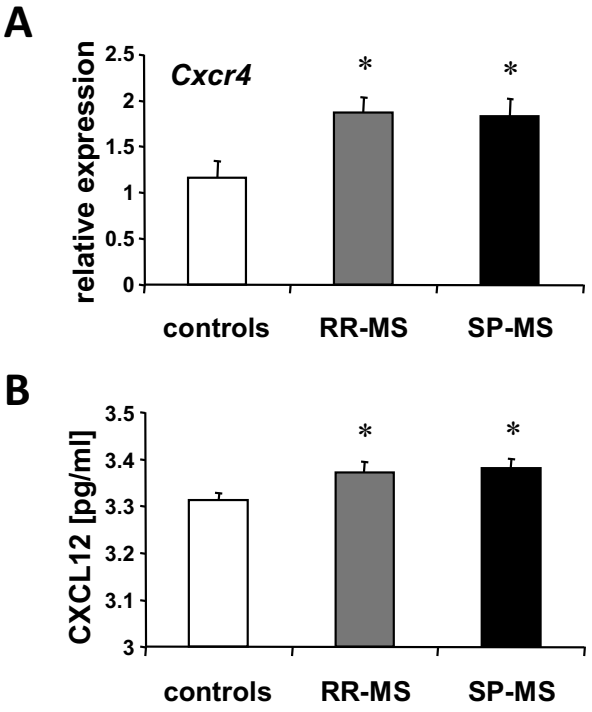

Fig. 3. *Cxcr4* expression in white blood cells and CXCL12 protein in serum of individuals with MS. (A) *Cxcr4* mRNA was quantified by real-time PCR from white blood cells of individuals with relapsing-remitting MS (RR-MS; gray bars, *n*=32), secondary chronic-progressive MS (SP-MS; black bars, *n*=22) and controls (white bars, *n*=25). Upregulation of *Cxcr4* in both patient groups compared to controls was observed (ANOVA, **P*<0.05). (B) CXCL12 serum levels were assessed by ELISA in individuals with RR-MS (gray bars, *n*=24), SP-MS (black bars, *n*=28) and controls (white bars, *n*=21). Increased serum levels of CXCL12 were measured in both MS groups compared to controls (ANOVA, **P*<0.05). Quantitative PCR results are expressed as $2^{-\Delta\Delta CT}$ values. Numbers are mean±s.e.m.

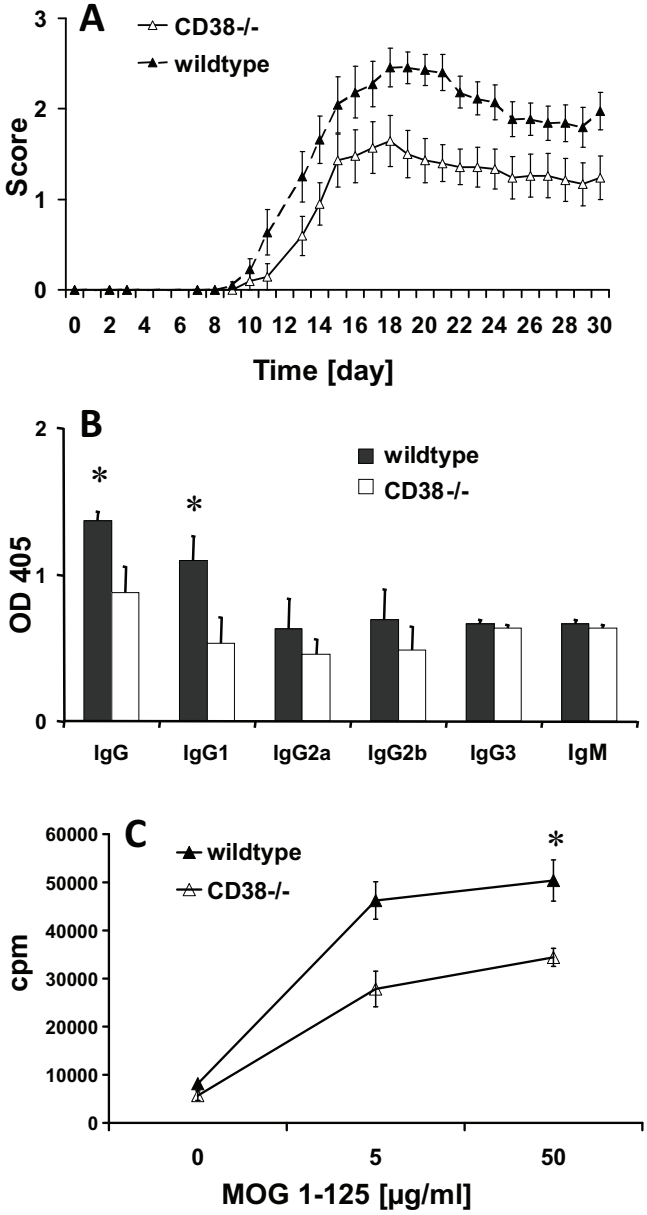

Fig. 4. EAE in B6.129P2-*Cd38*^{tm1Lnd}/J mice. (A) EAE was induced in female B6.129P2-*Cd38*^{tm1Lnd}/J mice (white triangles) and C57BL/6J 000664 controls (black triangles) with MOG 1-125 in CFA. On days 0 and 2 p.i., mice received an intravenous injection of 150 ng pertussis toxin. EAE was scored as follows: 0, no disease; 1, tail paralysis; 2, paraparesis; 3, paraplegia; 4, tetraparalysis; 5, moribund or dead. Immunization with the extracellular domain of MOG 1-125 resulted in B6.129P2-*Cd38*^{tm1Lnd}/J mice (*n*=22) with lower disease severity compared to C57BL/6J 000664 mice (*n*=21) (*t*-test, cumulative disease score, *P*=0.01). (B) Antibodies against MOG 1-125 were measured by ELISA as described (Weissert et al., 2001). B6.129P2-*Cd38*^{tm1Lnd}/J mice (white bars, *n*=4) had reduced IgG and IgG1 antibodies compared to C57BL/6J 000664 mice (black bars, *n*=4) (ANOVA, **P*<0.05) on day 12 p.i. (C) T-cell responses upon restimulation against MOG 1-125 from draining lymph nodes (LNs) on day 12 p.i. were reduced in B6.129P2-*Cd38*^{tm1Lnd}/J (white triangles, *n*=4) compared to C57BL/6J 000664 (black triangles, *n*=4) mice (*t*-test for stimulation with 50 µg/ml MOG 1-125, **P*=0.05). Numbers are mean±s.e.m.

expression and functional relevance of genes and their products expressed on lymphocytes after immunization with the encephalitogenic MOG 91-108 peptide in adjuvant, the non-encephalitogenic MOG 73-90 peptide in adjuvant, adjuvant alone or naive rats. Most interestingly, in the comparison of MOG 91-108 in adjuvant to MOG 73-90 in adjuvant immunized rats, compared to the other analyses, only a small number of genes were differentially expressed. These genes seem to be of major importance because they are genes involved in the encephalitogenic response leading to disease manifestation. From the overall expression data, we selected three genes that were upregulated in many comparisons: *Cxcr4*, *Cd38* and *Akt*. We performed functional studies regarding these genes in EAE and analyzed tissue samples from individuals with MS.

CXCR4 (CD184) is a seven-transmembrane G-coupled receptor expressed by a number of tissues, including cells of the immune system (Campbell et al., 2003). *Cxcr4*-knockout mice die *in utero* or perinatally and do not only have defects in the hematopoietic system (impairment of myeloid and B-cell generation, reduced proliferation of triple-negative and double-positive lymphocytes), but also in the circulatory system and in the CNS (Zou et al., 1998; Tachibana et al., 1998). Overexpression of CXCR4 on T cells induces their accumulation in the bone marrow and reduction of these cells in the peripheral blood. CXCR4 signaling leads to a prolonged protein kinase B (AKT) and extracellular signal-regulated kinase 2 activation in T cells. AKT activation promotes cell survival and can act as a co-stimulation for T-cell activation (Tilton et al., 2000). CXCR4 has only one known cognate ligand, which is CXCL12. CXCL12 is constitutively produced by stromal and endothelial cells. CXCL12 activates numerous signaling pathways, such as

Disease Models & Mechanisms (2016) 9, 1211-1220 doi:10.1242/dmm.025536

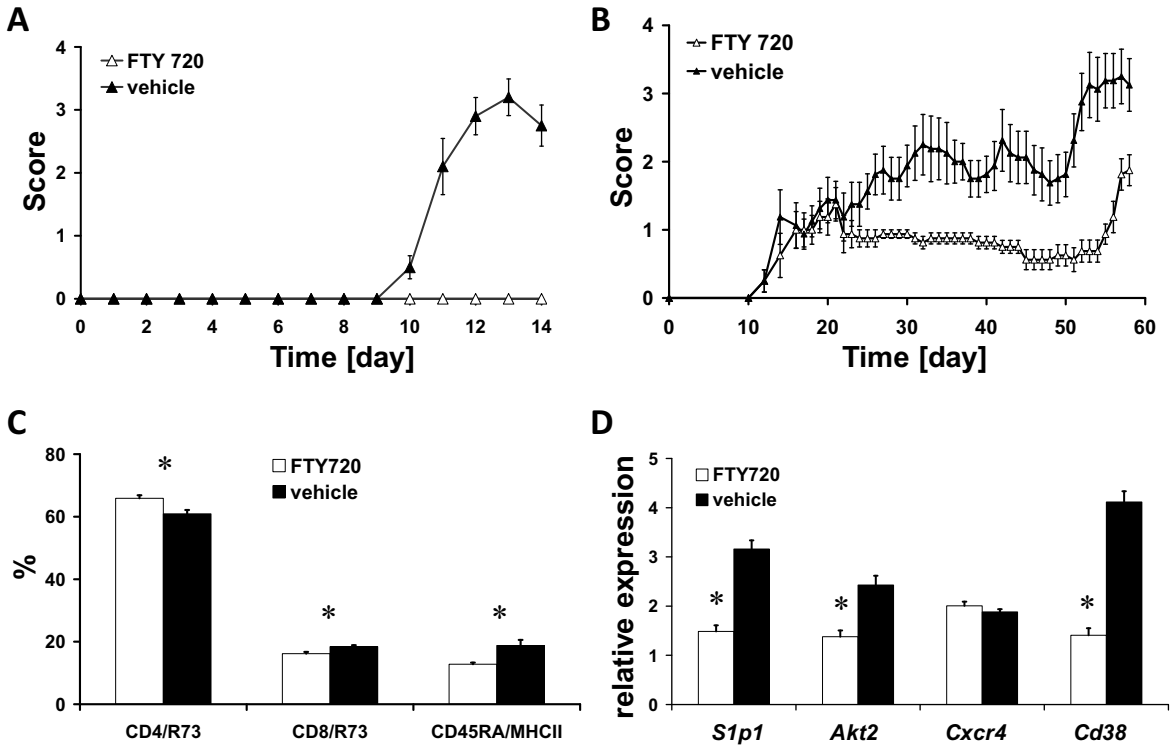

Fig. 5. Influence of FTY720 in EAE. (A) Female LEW.1AV1 (*RT1*^{av1}) rats were immunized with MOG 1-125 in CFA. EAE was scored as follows: 0, no disease; 1, tail paralysis; 2, paraparesis; 3, paraplegia; 4, tetraparalysis; 5, moribund or dead. FTY720 completely inhibited EAE in rats treated orally with 0.4 mg/kg body weight from day 0 p.i. daily (white triangles, *n*=10) as compared to vehicle (PBS)-treated controls (black triangles, *n*=10) (*t*-test, cumulative disease score, *P*<0.0001). (B) Female DA (*RT1*^{av1}) rats treated orally with 0.4 mg/kg body weight FTY720 daily starting on day 21 p.i. after a first bout of disease (white triangles, *n*=8) showed a reduced disease course compared to vehicle (PBS)-treated controls (black triangles, *n*=8) (*t*-test, cumulative disease score day 21-44 p.i., *P*=0.01). On day 44 p.i., rats were boosted with MOG 1-125 in CFA. Both groups relapsed but with a better outcome for the FTY720-treated group (*t*-test, cumulative disease score day 45-56 p.i., *P*<0.0001). (C) FACS analysis of cells from draining lymph nodes (LNs) demonstrated an increase in relative size of the CD4 T-cell compartment and a decrease in the size of the CD8 and B-cell compartment in FTY720-treated (white bars, *n*=10) rats compared to controls (black bars, *n*=9) (ANOVA, **P*<0.01) on day 14 p.i. (D) Expression of *S1p1* (*Edg1*), *Akt2*, *Cxcr4* and *Cd38* was assessed in FTY720-treated rats (white bars, *n*=9) compared to vehicle-treated controls (black bars, *n*=9) by quantitative PCR. FTY720 treatment led to downregulation of *S1p1* and *Akt2* as well as *Cd38*, but not of *Cxcr4* (ANOVA for all except *Cxcr4*, **P*<0.0001) on day 14 p.i. from cells derived from LNs. Results are expressed as $2^{-\Delta\Delta CT}$ values. Numbers are mean±s.e.m.

receptor-associated trimeric G proteins, phospholipase Cγ, PI3K and small G proteins (Pawig et al., 2015). Signaling through these receptors leads to an increase in the intracellular calcium concentration, cytoskeleton reorganization and cellular migration. Several modulating factors such as phosphatases, regulator of G-protein signaling, adaptor proteins and ubiquitin may affect signaling and/or chemotactic response of CXCR4 to its ligand (CXCL12). An important function of CXCR4/CXCL12 is the regulation of bone-marrow homeostasis and lymphocyte trafficking. Chemotaxis and integrin-mediated adhesion are the main cellular responses to CXCL12. *Cxcl12*-knockout mice display the same phenotype as *Cxcr4*-knockout mice (Nagasawa et al., 1996).

In autoimmunity there are indications that the interaction of CXCR4 and CXCL12 could be important. CXCL12 recruits B cells to inflamed glomeruli, in which these cells can produce autoantibodies (Balabanian et al., 2003). Also, in rheumatoid arthritis, CXCR4 and CXCL12 have been proposed to be important in the disease precipitation (Zhang et al., 2005). A role of CXCR4 and CXCL12 in EAE (Meiron et al., 2008; Kohler et al., 2008; McCandless et al., 2006) as well as in MS (Azin et al., 2012; Krumbholz et al., 2006) has been described.

Our data indicate that, also in MOG-induced EAE and possibly in MS, the interaction of CXCR4 and CXCL12 is of paramount importance for disease development. We found specific upregulation of *Cxcr4* on cells derived from LNs and eluted from the CNS of rats immunized with encephalitogenic MOG 91-108 peptide in comparison to controls. In addition, we measured upregulation of *Cxcl12* and *Cxcr4* in spinal cords in EAE rats compared to controls. CXCL12 is upregulated in the CNS of individuals with MS (Krumbholz et al., 2006 and our own unpublished observations). Together, the presented data would argue for a scenario in which LN-derived cells are, in the context of an encounter with an encephalitogenic antigen, activated and migrate towards CXCL12 in the CNS. This is further underscored by the fact that nitric oxide enhances lipopolysaccharide (LPS)-induced expression of CXCR4 and migration towards CXCL12 (Giordano et al., 2006).

CD38 is a membrane-associated type II glycoprotein that acts both as a receptor and enzyme (Cockayne et al., 1998; Kato et al., 1999; Salmi and Jalkanen, 2005). As an enzyme it catalyzes NAD+ into cyclic ADP-ribose and further into ADP-ribose. It also regulates Ca^{2+} levels from ryanodine receptor stores. CD38 is expressed on a variety of myeloid and lymphoid cells. CD38 ligation in B cells leads to tyrosine phosphorylation of several intracellular proteins such as Syk, p85 of phophatidylinositol-3 kinase and phospholipase C-γ (Silvennoinen et al., 1996). CD38 ligation in T cells results in phosphorylation of the Raf-1/MAP kinase and CD3-ζ/ZAP-70 signaling pathway (Zubiaur et al., 1997). Furthermore, it is involved in dendritic cell migration and adhesion between lymphocytes and endothelial cells (Partida-Sanchez et al., 2004). B6.129P2-*Cd38*^{tm1Lnd}/J mice show a slight reduction of

Disease Models & Mechanisms (2016) 9, 1211-1220 doi:10.1242/dmm.025536

antibody titers to T-cell-dependent antigens (Cockayne et al., 1998). Additionally, these mice had increased susceptibility to bacterial infections, which is thought to be caused by a defective chemotactic response of neutrophils towards bacteria, underscoring a role in innate immunity as well (Partida-Sanchez et al., 2001).

We induced EAE in *Cd38*-knockout mice (B6.129P2-*Cd38*^{tm1Lnd}/J) and controls. *Cd38*-knockout mice had a reduced disease severity and lower autoantibody and T-cell responses as compared to the controls. These findings show the importance of CD38 in EAE and possibly MS. This work forms the basis for further analysis of the involved cellular compartments and regulation of human disease (Mayo et al., 2008; Lischke et al., 2013).

FTY720 is a potent drug that affects lymphocyte trafficking and homing. Our studies and studies by others (Brinkmann et al., 2002; Balatoni et al., 2007) showed a strong beneficial effect of FTY720 on EAE under various experimental settings. The drug was approved for treatment of MS (Kappos et al., 2010). We demonstrate that treatment of MOG-induced EAE with FTY720 impacts the gene expression of the genes that are involved in encephalitogenic immune responses. This further validates our approach. We measured changes in expression of *S1P1*, *Akt2* and *Cd38*. Interestingly, no changes in expression of *Cxcr4* was observed. The reason for this is not fully understood and deserves further investigations.

In conclusion, in this study we have identified genes that are involved not only in raising autoantigen-specific immune responses but which constitute encephalitogenicity. The immunization with encephalitogenic peptides induces a network of genes involved in activation and migration of lymphocytes. Based on this platform, we have established the paramount importance of G-coupled proteins in encephalitogenicity of adaptive immune responses. We speculate that similar involvement might operate also in other autoimmune diseases and possibly in transplant rejection, thereby establishing common mechanisms. These pathways might be valuable targets of therapeutic approaches as we have shown attenuation of EAE after treatment with FTY720 or reduced EAE severity in CD38-deficient mice. These findings not only validate our gene expression data, but also underscore the importance of the rat EAE model in translational medicine.

MATERIALS AND METHODS

Animals and EAE induction

Female rats or mice, 10-14 weeks of age, were used in all experiments. LEW.1AV1 (*RT1*^{av1}) rats were obtained from Hans Hedrich (Central Animal Laboratory, Hannover Medical School, Hannover, Germany) and DA (*RT1*^{av1}) rats were obtained from Harlan Winkelmann (Borchen, Germany). Female B6.129P2-*Cd38*^{tm1Lnd}/J mice and the appropriate controls (C57BL/6J 000664) were purchased from the Jackson Laboratory (Bar Harbor, USA).

Animals were bred and kept under specific pathogen-free conditions. Animals were injected intradermally at the base of the tail (rats) or both flanks (mice) with 100 µg of MOG 91-108 (rats) or 50 µg of rat recombinant MOG 1-125 (rats) or 100 µg MOG 35-55 (mice) or 20 µg rat recombinant MOG 1-125 (mice). The antigens in a total volume of 100 µl were mixed with 100 µl of CFA (1:1). A total of 100 µl of CFA consisted of IFA (Sigma-Aldrich, St Louis, MO) and 500 µg for rats or 400 µg for mice of heat-inactivated *Mycobacterium tuberculosis* (strain H37 RA; Difco Laboratories, Detroit, MI) (Weissert, 2016). Mice additionally received 100 ng of pertussis toxin (Calbiochem, Darmstadt, Germany) on day 0 and 2 intravenously. Some groups of rats were also injected with 100 µl IFA mixed with 100 µl MOG 1-125 in PBS (50 µg) without the addition of *Mycobacterium tuberculosis* or with IFA or CFA alone. The clinical scoring was as follows: 0=no illness; 1=tail weakness or paralysis; 2=hind-leg paraparesis or hemiparesis; 3=hind-leg paralysis or hemiparalysis; 4=tetraparesis or moribund. All experiments were approved by the regional board in Tübingen, Germany.

Human samples

Blood samples were obtained after consent from individuals with MS and controls. The characteristics of the MS individuals and controls are indicated in Tables S6 and S7. The research was approved by the Ethics Committee of the University of Tübingen in Germany (Permission 125/2001).

Isolation of CNS-infiltrating cells

Infiltrating cells from the CNS were prepared as described before (Weissert et al., 1998a, 2001). In brief, rats were perfused with cold PBS, and brains and spinal cords were dissected out on day 12 p.i. Subsequently, brains and spinal cords were homogenized in 10 ml 50% Percoll/0.1% BSA/1% glucose (Amersham Pharmacia Biotech) containing 500 U DNase type I (Life Technologies). Ten ml of 50% Percoll was added to each sample after homogenization. A discontinuous Percoll gradient was obtained by adding 7 ml of 63% Percoll below and 20 ml of 30% Percoll above the sample. Samples were centrifuged for 40 min at 1000 ***g*** at 4°C. Lymphocytes were collected from the 63/50% Percoll interface. The cells were subsequently washed twice in 15-25 ml PBS with centrifugation at 600 ***g*** for 15 min at 4°C.

Isolation of mononuclear cells from lymph nodes and spleens

Draining inguinal LNs and spleens were dissected out under deep anesthesia. LNs were disrupted and mononuclear cells (MNCs) washed twice in Dulbecco's modified Eagle's medium (DMEM; Life Technologies, Paisley, UK), resuspended in complete medium (CM) containing DMEM supplemented with 5% fetal calf serum (PAA Laboratories Linz, Austria), 1% penicillin/streptomycin (Life Technologies), 1% glutamine (Life Technologies) and 50 µM 2-mercaptoethanol (Life Technologies), and flushed through a 70-µm plastic strainer (Falcon; BD Biosciences, Franklin Lakes, NJ). MNCs from spleen were prepared in the same way as from LNs with the difference that red blood cells were lysed with lysis buffer consisting of 0.15 M NH_4Cl, 10 mM $KHCO_3$ and 0.1 mM Na_2 EDTA adjusted to pH 7.4. $CD4^+$ cells were isolated by anti-rat CD4 microbeads using MACS technology (Miltenyi Biotech, Bergisch Gladbach, Germany) according to the manufacturer's instruction.

$CD4^+$ cell purification

$CD4^+$ cells from the LNs were purified by MACS (Miltenyi Biotech, Bergisch Gladbach, Germany) and subsequently analyzed by Affymetrix gene array for differential gene expression.

Spinal cord tissue

From PBS-perfused naive rats or in DA rats immunized with either IFA, CFA, MOG 1-125 in IFA or MOG 1-125 in CFA, spinal cord tissue was dissected and homogenized and subsequently assessed for mRNA expression.

RNA preparation

Total RNA of brain-infiltrating leukocytes or lymphocytes or spinal cord tissue was isolated by using an RNeasy kit (Qiagen, Hilden, Germany) according to the manufacturer's instructions. The RNA quality was analyzed with a Bioanalyser 2100 (Agilent, Palo Alto, CA).

Microarrays

Affymetrix microarrays of the type RG U34 A (Affymetrix Inc., Santa Clara, CA) representing approximately 7000 full-length genes and 1000 expressed sequence tag (EST) clusters were used. For the purified $CD4^+$ cells, the rat expression set 230A (Affymetrix) containing about 30,000 features was used. For each array, samples from at least three rats were pooled. Biotin-labeled cRNA was prepared and hybridized to the arrays. In brief, double-stranded cDNA was synthesized from whole RNA using a superscript choice kit (Invitrogen) with a T7-(dT)24 primer (Metabion) and *in vitro* transcribed into biotin-labeled cRNA. After hybridization, gene

Disease Models & Mechanisms (2016) 9, 1211-1220 doi:10.1242/dmm.025536

arrays were washed and stained by a fluidics station (Affymetrix) and scanned by a confocal laser scanning microscope (Agilent).

The data were analyzed using the microarray suite software, micro DB, and data-mining tool (Affymetrix). Only genes and ESTs that were 'present' and gave a difference call of either 'increase' or 'decrease' according to the Affymetrix software were included in further analysis. The extent of differential expression is expressed as an SLR. For the tables, the cut-off was set to an SLR of 1 signifying a twofold change in expression. Doubles, ESTs and sequences not corresponding to a gene were not included in the tables.

Real-time PCR

To avoid amplification/detection of contaminating genomic DNA, extracted RNA was treated with RNase free DNase (Promega, Madison, WI). Subsequently, cDNA was synthesized by reverse transcription with Moloney murine leukemia virus reverse transcriptase and random pdN6 primers in the presence of RNase inhibitor (Promega). Amplification was performed on an Applied Biosystems Prism 7000 Sequence Detection System (Applied Biosystems, Foster City, CA) using a SYBR green protocol. Results were expressed as $2^{-\Delta\Delta CT}$ values. The primer sequences 5′ to 3′ were as follows:

Rat primers

Gapdh: forward: GGTTGTCTCCTGTGACTTCAA
reverse: CATACCAGGAAATGAGCTTCAC
S1p1: forward: TAGCCGCAGCAAATCAGAC
reverse: GCAGCAGTGGAGAAAGAGAGA
Cxcr4: forward: GATGGTGGTGTTCCAGTTCC
reverse: CAGCTTGGAGATGATGATGC
Cxcl12: forward: CGATTCTTTGAGAGCCATGT
reverse: AGGGCACAGTTTGGAGTGTT
Cd38: forward: AGGACACACTGCTGGGCTAT
reverse: CAGGGTTGTTGGGACAATTT
Akt2: forward: GAAGACTGAGAGGCCACGAC
reverse: GGGAGCCACACTTGTAATCC

Human primers

h18s: forward: CGGCTACCACATCCAAGGAA
reverse: GCTGGAATTACCGCGGCT
Cxcr4: forward: CATCAGTCTGGACCGCTACC
reverse: GGATCCAGACGCCAACATAG.

FACS

FITC-conjugated monoclonal antibody (mAb) against CD45RA (OX-33) and TCRAB (R73) and phycoerythrin (PE)-conjugated mAb against CD4 (OX-35) and MHC II (OX-6) and appropriate isotype controls were purchased from Becton Dickinson (Heidelberg, Germany). Flow cytometry was performed on a FACScalibur running with Cellquest software (Becton Dickinson). Cells were gated on the lymphocyte population in the forward scatter (FSC)-side scatter (SSC) dot plot. For data analysis, Flowing Software 2.5.1 (Turku Center for Biotechnology, Finland) was used.

ELISA

Serum taken at the time point of euthanasia was subject to an anti-MOG autoantibody ELISA. ELISA plates (96-well; Nunc, Roskilde, Denmark) were coated with 2.5 µg/ml (100 µl/well) MOG 1-125 overnight at 4°C. Plates were washed with PBS/0.05% Tween 20 and blocked with milk powder for 1 h at room temperature. After washing, diluted serum samples were added and plates were incubated for 1 h at room temperature. Then, plates were washed and rabbit anti-mouse antiserum (IgG, IgG1, IgG2a, IgG2b, IgG3, IgM; Nordic, Tilburg, The Netherlands) was added and incubated for 1 h at room temperature. Plates were washed prior to the addition of peroxidase-conjugated goat anti-rabbit antiserum (Nordic) diluted in PBS/0.05% Tween 20. After 30 min incubation, plates were washed and bound antibodies were visualized by addition of 2,2′azino-bis (3-ethylbenzothiazoline-6-sulphonic acid) (ABTS) (Roche Diagnostics, Mannheim, Germany). After 15 min of incubation, optical density was read at 405 nm.

ELISA with human serum was performed according to the instructions of the manufacturer [Quantikine human SDF1alpha Immunoassay (R&D Systems, Minneapolis, MN)].

Proliferation assay

Cells from draining LNs were prepared as described above and cultured in the presence of rrMOG in 96-well plates as described by Weissert et al. (1998b). Cells were cultured for 48 h and pulsed with 1 µCi [^{3}H]thymidine for the last 18 h. The incorporation of [^{3}H]thymidine was measured using a beta-scintillation counter.

FTY720 treatment

Rats were treated with FTY720 (generous gift of Novartis AG, Switzerland) and received a daily dose of 0.4 mg/kg body weight in sterile water by oral gavage as described (Balatoni et al., 2007).

This article is part of a special subject collection 'Spotlight on Rat: Translational Impact', guest edited by Tim Aitman and Aron Geurts. See related articles in this collection at http://dmm.biologists.org/collection/rat-disease-model.

Acknowledgements

We thank Thomas Weiss and Kerstin Stuck for excellent technical assistance.

Competing interests

The authors declare no competing or financial interests.

Author contributions

M.M.H. performed the gene arrays, data analysis, target validation in rats and revised the paper. S.B. performed the gene arrays, data analysis and the target validation. B.G. did the work on CD38 in mice. K.M.S. performed target validation studies in rats and analyzed the data. A.B. performed studies in individuals with MS and controls. R.W. designed the study, raised the funding, performed the data analysis, and wrote and revised the paper.

Funding

This study was supported by grants from the Interdisciplinary Centre for Clinical Research (Bundesministerium für Bildung und Forschung) (Fö. 01KS9602), and German Research Foundation (Deutsche Forschungsgemeinschaft) to R.W. (DFG We 1947).

Supplementary information

Supplementary information available online at
http://dmm.biologists.org/lookup/doi/10.1242/dmm.025536.supplemental

References

Azin, H., Vazirinejad, R., Ahmadabadi, B. N., Khorramdelazad, H., Zarandi, E. R., Arababadi, M. K., Karimabad, M. N., Shamsizadeh, A., Rafatpanah, H. and Hassanshahi, G. (2012). The SDF-1 3′a genetic variation of the chemokine SDF-1alpha (CXCL12) in parallel with its increased circulating levels is associated with susceptibility to MS: a study on Iranian multiple sclerosis patients. *J. Mol. Neurosci.* **47**, 431-436.

Balabanian, K., Couderc, J., Bouchet-Delbos, L., Amara, A., Berrebi, D., Foussat, A., Baleux, F., Portier, A., Durand-Gasselin, I., Coffman, R. L. et al. (2003). Role of the chemokine stromal cell-derived factor 1 in autoantibody production and nephritis in murine lupus. *J. Immunol.* **170**, 3392-3400.

Balatoni, B., Storch, M. K., Swoboda, E.-M., Schonborn, V., Koziel, A., Lambrou, G. N., Hiestand, P. C., Weissert, R. and Foster, C. A. (2007). FTY720 sustains and restores neuronal function in the DA rat model of MOG-induced experimental autoimmune encephalomyelitis. *Brain Res. Bull.* **74**, 307-316.

Brinkmann, V., Davis, M. D., Heise, C. E., Albert, R., Cottens, S., Hof, R., Bruns, C., Prieschl, E., Baumruker, T., Hiestand, P. et al. (2002). The immune modulator FTY720 targets sphingosine 1-phosphate receptors. *J. Biol. Chem.* **277**, 21453-21457.

Campbell, D. J., Kim, C. H. and Butcher, E. C. (2003). Chemokines in the systemic organization of immunity. *Immunol. Rev.* **195**, 58-71.

Cockayne, D. A., Muchamuel, T., Grimaldi, J. C., Muller-Steffner, H., Randall, T. D., Lund, F. E., Murray, R., Schuber, F. and Howard, M. C. (1998). Mice deficient for the ecto-nicotinamide adenine dinucleotide glycohydrolase CD38 exhibit altered humoral immune responses. *Blood* **92**, 1324-1333.

Cyster, J. G. (2005). Chemokines, sphingosine-1-phosphate, and cell migration in secondary lymphoid organs. *Annu. Rev. Immunol.* **23**, 127-159.

Dumas, A., Amiable, N., De Rivero Vaccari, J. P., Chae, J. J., Keane, R. W., Lacroix, S. and Vallieres, L. (2014). The inflammasome pyrin contributes to pertussis toxin-induced IL-1beta synthesis, neutrophil intravascular crawling and autoimmune encephalomyelitis. *PLoS Pathog.* **10**, e1004150.

Genain, C. P., Nguyen, M. H., Letvin, N. L., Pearl, R., Davis, R. L., Adelman, M., Lees, M. B., Linington, C. and Hauser, S. L. (1995). Antibody facilitation of multiple sclerosis-like lesions in a nonhuman primate. *J. Clin. Invest.* **96**, 2966-2974.

Giordano, D., Magaletti, D. M. and Clark, E. A. (2006). Nitric oxide and cGMP protein kinase (cGK) regulate dendritic-cell migration toward the lymph-node-directing chemokine CCL19. *Blood* **107**, 1537-1545.

Hur, E. M., Youssef, S., Haws, M. E., Zhang, S. Y., Sobel, R. A. and Steinman, L. (2007). Osteopontin-induced relapse and progression of autoimmune brain disease through enhanced survival of activated T cells. *Nat. Immunol.* **8**, 74-83.

Kappos, L., Radue, E.-W., O'connor, P., Polman, C., Hohlfeld, R., Calabresi, P., Selmaj, K., Agoropoulou, C., Leyk, M., Zhang-Auberson, L. et al.; FREEDOMS Study Group. (2010). A placebo-controlled trial of oral fingolimod in relapsing multiple sclerosis. *N. Engl. J. Med.* **362**, 387-401.

Kato, I., Yamamoto, Y., Fujimura, M., Noguchi, N., Takasawa, S. and Okamoto, H. (1999). CD38 disruption impairs glucose-induced increases in cyclic ADP-ribose, [Ca2+]i, and insulin secretion. *J. Biol. Chem.* **274**, 1869-1872.

Kohler, R. E., Comerford, I., Townley, S., Haylock-Jacobs, S., Clark-Lewis, I. and Mccoll, S. R. (2008). Antagonism of the chemokine receptors CXCR3 and CXCR4 reduces the pathology of experimental autoimmune encephalomyelitis. *Brain Pathol.* **18**, 504-516.

Kornek, B., Storch, M. K., Weissert, R., Wallstroem, E., Stefferl, A., Olsson, T., Linington, C., Schmidbauer, M. and Lassmann, H. (2000). Multiple sclerosis and chronic autoimmune encephalomyelitis: a comparative quantitative study of axonal injury in active, inactive, and remyelinated lesions. *Am. J. Pathol.* **157**, 267-276.

Krumbholz, M., Theil, D., Cepok, S., Hemmer, B., Kivisakk, P., Ransohoff, R. M., Hofbauer, M., Farina, C., Derfuss, T., Hartle, C. et al. (2006). Chemokines in multiple sclerosis: CXCL12 and CXCL13 up-regulation is differentially linked to CNS immune cell recruitment. *Brain* **129**, 200-211.

Lee, M.-J., Thangada, S., Paik, J.-H., Sapkota, G. P., Ancellin, N., Chae, S.-S., Wu, M., Morales-Ruiz, M., Sessa, W. C., Alessi, D. R. et al. (2001). Akt-mediated phosphorylation of the G protein-coupled receptor EDG-1 is required for endothelial cell chemotaxis. *Mol. Cell* **8**, 693-704.

Lischke, T., Heesch, K., Schumacher, V., Schneider, M., Haag, F., Koch-Nolte, F. and Mittrucker, H.-W. (2013). CD38 controls the innate immune response against Listeria monocytogenes. *Infect. Immun.* **81**, 4091-4099.

Lucchinetti, C., Bruck, W., Parisi, J., Scheithauer, B., Rodriguez, M. and Lassmann, H. (2000). Heterogeneity of multiple sclerosis lesions: implications for the pathogenesis of demyelination. *Ann. Neurol.* **47**, 707-717.

Mandala, S., Hajdu, R., Bergstrom, J., Quackenbush, E., Xie, J., Milligan, J., Thornton, R., Shei, G.-J., Card, D., Keohane, C. et al. (2002). Alteration of lymphocyte trafficking by sphingosine-1-phosphate receptor agonists. *Science* **296**, 346-349.

Mathey, E., Breithaupt, C., Schubart, A. S. and Linington, C. (2004). Commentary: sorting the wheat from the chaff: identifying demyelinating components of the myelin oligodendrocyte glycoprotein (MOG)-specific autoantibody repertoire. *Eur. J. Immunol.* **34**, 2065-2071.

Matloubian, M., Lo, C. G., Cinamon, G., Lesneski, M. J., Xu, Y., Brinkmann, V., Allende, M. L., Proia, R. L. and Cyster, J. G. (2004). Lymphocyte egress from thymus and peripheral lymphoid organs is dependent on S1P receptor 1. *Nature* **427**, 355-360.

Mayo, L., Jacob-Hirsch, J., Amariglio, N., Rechavi, G., Moutin, M.-J., Lund, F. E. and Stein, R. (2008). Dual role of CD38 in microglial activation and activation-induced cell death. *J. Immunol.* **181**, 92-103.

Mccandless, E. E., Wang, Q., Woerner, B. M., Harper, J. M. and Klein, R. S. (2006). CXCL12 limits inflammation by localizing mononuclear infiltrates to the perivascular space during experimental autoimmune encephalomyelitis. *J. Immunol.* **177**, 8053-8064.

Meiron, M., Zohar, Y., Anunu, R., Wildbaum, G. and Karin, N. (2008). CXCL12 (SDF-1alpha) suppresses ongoing experimental autoimmune encephalomyelitis by selecting antigen-specific regulatory T cells. *J. Exp. Med.* **205**, 2643-2655.

Mills, K. H. (2011). TLR-dependent T cell activation in autoimmunity. *Nat. Rev. Immunol.* **11**, 807-822.

Nagasawa, T., Nakajima, T., Tachibana, K., Iizasa, H., Bleul, C. C., Yoshie, O., Matsushima, K., Yoshida, N., Springer, T. A. and Kishimoto, T. (1996). Molecular cloning and characterization of a murine pre-B-cell growth-stimulating factor/stromal cell-derived factor 1 receptor, a murine homolog of the human immunodeficiency virus 1 entry coreceptor fusin. *Proc. Natl. Acad. Sci. USA* **93**, 14726-14729.

Noseworthy, J. H., Lucchinetti, C., Rodriguez, M. and Weinshenker, B. G. (2000). Multiple sclerosis. *N. Engl. J. Med.* **343**, 938-952.

Partida-Sanchez, S., Cockayne, D. A., Monard, S., Jacobson, E. L., Oppenheimer, N., Garvy, B., Kusser, K., Goodrich, S., Howard, M., Harmsen, A. et al. (2001). Cyclic ADP-ribose production by CD38 regulates intracellular calcium release, extracellular calcium influx and chemotaxis in neutrophils and is required for bacterial clearance in vivo. *Nat. Med.* **7**, 1209-1216.

Partida-Sanchez, S., Goodrich, S., Kusser, K., Oppenheimer, N., Randall, T. D. and Lund, F. E. (2004). Regulation of dendritic cell trafficking by the ADP-ribosyl cyclase CD38: impact on the development of humoral immunity. *Immunity* **20**, 279-291.

Pawig, L., Klasen, C., Weber, C., Bernhagen, J. and Noels, H. (2015). Diversity and inter-connections in the CXCR4 chemokine receptor/ligand family: molecular perspectives. *Front. Immunol.* **6**, 429.

Riedhammer, C. and Weissert, R. (2015). Antigen presentation, autoantigens, and immune regulation in multiple sclerosis and other autoimmune diseases. *Front. Immunol.* **6**, 322.

Salmi, M. and Jalkanen, S. (2005). Cell-surface enzymes in control of leukocyte trafficking. *Nat. Rev. Immunol.* **5**, 760-771.

Silvennoinen, O., Nishigaki, H., Kitanaka, A., Kumagai, M., Ito, C., Malavasi, F., Lin, Q., Conley, M. E. and Campana, D. (1996). CD38 signal transduction in human B cell precursors. Rapid induction of tyrosine phosphorylation, activation of syk tyrosine kinase, and phosphorylation of phospholipase C-gamma and phosphatidylinositol 3-kinase. *J. Immunol.* **156**, 100-107.

Storch, M. K., Stefferl, A., Brehm, U., Weissert, R., Wallstrom, E., Kerschensteiner, M., Olsson, T., Linington, C. and Lassmann, H. (1998). Autoimmunity to myelin oligodendrocyte glycoprotein in rats mimics the spectrum of multiple sclerosis pathology. *Brain Pathol.* **8**, 681-694.

Tachibana, K., Hirota, S., Iizasa, H., Yoshida, H., Kawabata, K., Kataoka, Y., Kitamura, Y., Matsushima, K., Yoshida, N., Nishikawa, S.-I. et al. (1998). The chemokine receptor CXCR4 is essential for vascularization of the gastrointestinal tract. *Nature* **393**, 591-594.

Tilton, B., Ho, L., Oberlin, E., Loetscher, P., Baleux, F., Clark-Lewis, I. and Thelen, M. (2000). Signal transduction by CXC chemokine receptor 4. Stromal cell-derived factor 1 stimulates prolonged protein kinase B and extracellular signal-regulated kinase 2 activation in T lymphocytes. *J. Exp. Med.* **192**, 313-324.

Weissert, R. (2013). The immune pathogenesis of multiple sclerosis. *J. Neuroimmune Pharmacol.* **8**, 857-866.

Weissert, R. (2016). Actively induced experimental autoimmune encephalomyelitis in rats. *Methods Mol. Biol.* **1304**, 161-169.

Weissert, R., Svenningsson, A., Lobell, A., De Graaf, K. L., Andersson, R. and Olsson, T. (1998a). Molecular and genetic requirements for preferential recruitment of TCRBV8S2+ T cells in Lewis rat experimental autoimmune encephalomyelitis. *J. Immunol.* **160**, 681-690.

Weissert, R., Wallstrom, E., Storch, M. K., Stefferl, A., Lorentzen, J., Lassmann, H., Linington, C. and Olsson, T. (1998b). MHC haplotype-dependent regulation of MOG-induced EAE in rats. *J. Clin. Invest.* **102**, 1265-1273.

Weissert, R., De Graaf, K. L., Storch, M. K., Barth, S., Linington, C., Lassmann, H. and Olsson, T. (2001). MHC class II-regulated central nervous system autoaggression and T cell responses in peripheral lymphoid tissues are dissociated in myelin oligodendrocyte glycoprotein-induced experimental autoimmune encephalomyelitis. *J. Immunol.* **166**, 7588-7599.

Zhang, X., Nakajima, T., Goronzy, J. J. and Weyand, C. M. (2005). Tissue trafficking patterns of effector memory CD4+ T cells in rheumatoid arthritis. *Arthritis Rheum.* **52**, 3839-3849.

Zou, Y.-R., Kottmann, A. H., Kuroda, M., Taniuchi, I. and Littman, D. R. (1998). Function of the chemokine receptor CXCR4 in haematopoiesis and in cerebellar development. *Nature* **393**, 595-599.

Zubiaur, M., Izquierdo, M., Terhorst, C., Malavasi, F. and Sancho, J. (1997). CD38 ligation results in activation of the Raf-1/mitogen-activated protein kinase and the CD3-zeta/zeta-associated protein-70 signaling pathways in Jurkat T lymphocytes. *J. Immunol.* **159**, 193-205.

Table S1. Genes with decreased expression in lymphnode cells of LEW.1AV1 (RT1^{av1}) rats. The analysis was performed as described in Table 1.

Gene symbol	Gene Title	Affymetrix Probe Set ID	MOG 91-108 vs naive percentage	MOG 91-108 vs naive average SLR	MOG 91-108 vs CFA percentage	MOG 91-108 vs CFA average SLR	MOG 91-108 vs MOG73-90 percentage	MOG 91-108 vs MOG73-90 average SLR
Hmgcs1	3-hydroxy-3-methylglutaryl-Co A synthase 1	rc_AI177004_	90	-1.21	50	-0.97		
Idi1	isopentenyl-diphosphate delta isomerase	AF003835_at	50	-1.03	50	-1.04		
Ret	ret proto-oncogene	rc_AI639318_	80	-1.22				
Atrx	alpha thalassemia (RAD54 homolog, S.cerevisiae)	D64059_at	70	-1.29				
Rasgrp1	RAS guanyl releasing protein 1	AF081196_at	60	-1.18				
Nap65	Nopp140 associated protein	AF069782_at	50	-0.75				
Kras2	Kirsten rat sarcoma viral oncogene hom. 2	U09793_at	50	-0.74				
Cyb5	cytochrome b5	rc_AA945054_s_at			60	-1.70		
Gerp95	GERp95	rc_H31692_at			50	-0.89		
Stat3	signal transducer and activator of transcription 3	X91810_at					100	-1.15
Rasgrp1	RAS guanyl releasing protein 1	AF081196_at					80	-1.60
Nos2	nitric oxide synthase 2, inducible	U48829_s_at					80	-1.54
Col1a1	collagen, type 1, alpha 1	Z78279_at					80	-1.11
Cyb5	cytochrome b5	rc_AA945054_s_at					60	-1.87
Ets1	v-ets erythroblastosis virus E26 oncogene hom. 1	rc_AI175900_g_at					60	-1.32
Cat	catalase	M11670_at					60	-1.16
Pdpk1	3-phosphoinositide dependent protein kinase-1	Y15748_at					60	-1.15
Nap65	Nopp140 associated protein	AF069782_at					60	-1.09
Hk1	hexokinase 1	AFFX_Rat_Hexokinase_5_at					60	-1.00
Sparc	secreted acidic cysteine rich glycoprotein	Y13714_at					60	-0.94
Ptb	polypyrimidine tract binding protein	X74565cds_g_at					60	-0.89
Hbb	hemoglobin beta chain complex	M94918mRNA_f_at					60	-0.86

Table S2. Genes with increased expression in CNS- infiltrating cells of LEW.1AV1 (RT1^{av1}) rats. Comparisons of microarrays of brain infiltrating cells derived from LEW.1AV1 (RT1^{av1}) rats after immunization with MOG 91-108 (pooled samples, n=2 gene chips), MOG 73-90 (pooled samples, n=2 gene chips) and CFA alone (pooled samples, n=1 gene chip) resulted in many more genes being differentially expressed as compared to the analysis of lymph node cells. The analysis was performed as described in Table 1.

Gene Symbol	Gene Title	Probe Set ID	MOG 91-108 vs CFA and MOG 73-90 percentage	MOG 91-108 vs CFA and MOG 73-90 average SLR
Crem	cAMP responsive element modulator	S66024_at	100	5,33
Timp1	tissue inhibitor of metalloproteinase 1	rc_AI169327_g_at	100	5,19
Ifng	interferon gamma	AF010466_s_at	100	4,9
Ass	arginosuccinate synthetase	X12459_at	100	4,76
Cd38	CD38 antigen	rc_AA819187_s_at	100	4,5
Arg1	arginase 1	J02720_at	100	4,4
Cxcl10	chemokine (C-X-C motif) ligand 10	U17035_s_at	100	3,51
Cd2	CD2 antigen	X05111_at	100	3,51
Gbp2	guanylate binding protein 2, interferon-inducible	M80367_at	100	3,5
Nos2	nitric oxide synthase 2, inducible	D44591_s_at	100	3,49
Tnfrsf4	tumor necrosis factor receptor superfamily, member 4	X17037cds_at	100	3,36
Tcrb	Rat T-cell receptor active beta-chain C-region mRNA	X14319cds_g_at	100	3,34
Stat1	signal transducer and activator of transcription 1	rc_AA892553_at	100	3,3
Psmb9	proteosome (prosome, macropain) subunit, beta type 9	D10757_at	100	3,25
Cd3d	CD3 antigen delta polypeptide	X53430_at	100	3,23
Il2ra	interleukin 2 receptor, alpha chain	M55049_at	100	3,02
Prkch	protein kinase C, eta	X68400_at	100	2,81
Fabp5	fatty acid binding protein 5, epidermal	S69874_s_at	100	2,74
Lck	lymphocyte protein tyrosine kinase	rc_AA800684_at	100	2,72
Prf1	perforin 1 (pore forming protein)	M33605_at	100	2,71
Cd14	CD14 antigen	AF087943_s_at	100	2,7
Hmgcr	3-hydroxy-3-methylglutaryl-Coenzyme A reductase	M29249cds_at	100	2,69
Il1b	interleukin 1 beta	M98820_g_at	100	2,65
Il3	interleukin 3	X03914mergedCDS	100	2,57
Pde4d	phosphodiesterase 4D	L27060_at	100	2,55
RT1.S3	MHC class Ib RT1.S3	rc_AI235890_s_at	100	2,53
Tap1	transporter 1, ATP-binding cassette, sub-family B (MDR/TAP)	X57523_g_at	100	2,52
Gzmc	granzyme C	U57062_at	100	2,52
Vcam1	vascular cell adhesion molecule 1	M84488_at	100	2,5
Irf1	interferon regulatory factor 1	M34253_at	100	2,44
Il2rb	interleukin 2 receptor, beta chain	M55050_at	100	2,4
Cd3z	CD3 antigen, zeta polypeptide	D13555_at	100	2,39
RT1-Aw2	RT1 class Ib, locus Aw2	M10094_at	100	2,34
Hrasls3	HRAS like suppressor	X76453_at	100	2,3
Fhl2	four and a half LIM domains 2	rc_AA891527_at	100	2,28
Psme2	protease (prosome, macropain) 28 subunit, beta	D45250_s_at	100	2,27
Cd5	CD5 antigen	D10728_at	100	2,25
Ets1	v-ets erythroblastosis virus E26 oncogene homolog 1 (avian)	rc_AI175900_g_at	100	2,2
Lgals1	lectin, galactose binding, soluble 1	rc_AI172064_at	100	2,16
Trib3	tribbles homolog 3 (Drosophila)	rc_H31287_g_at	100	2,13
RT1-Bb	RT1 class II, locus Bb	M36151cds_s_at	100	2,13
RT1-Bb /// RT1	RT1 class II, locus Bb /arrestin, beta 2, pseudogene	X53054_at	100	2,11
Fkbp1a	FK506-binding protein 1a	rc_AI228738_s_at	100	2,09
Cxcl1	chemokine (C-X-C motif) ligand 1	D11445exon#1-4_s_	100	2,07
Psmb8	proteosome (prosome, macropain) subunit, beta type 8	D10729_s_at	100	2,05

Table S3. Genes with decreased expression in CNS infiltrating cells of LEW.1AV1 (RT1^{av1}) rats. The analysis was performed as described in Table 1.

Gene Symbol	Gene Title	Probe Set ID	MOG 91-108 vs CFA and MOG 73-90 percentage	MOG 91-108 vs CFA and MOG 73-90 average SLR
Enpp2	ectonucleotide pyrophosphatase/phosphodiesterase 2	D28560_at	100	-3,77
Syn2	synapsin II	rc_AI145494_at	100	-3,29
Atp2b3	ATPase, Ca++ transporting, plasma membrane 3	J05087_at	100	-3,27
Cgef2	cAMP-regulated guanine nucleotide exchange factor II	U78517_at	100	-3,25
Slc12a5	solute carrier family 12	U55816_at	100	-3,24
Mapt	microtubule-associated protein tau	rc_AI227608_s_at	100	-3,16
Enpp2	ectonucleotide pyrophosphatase/phosphodiesterase 2	D28560_g_at	100	-3,13
Ttr	transthyretin	rc_AA945169_at	100	-3,04
Scn1a	sodium channel, voltage-gated, type 1, alpha polypeptide	M22253_at	100	-3,02
Pdpk1	3-phosphoinositide dependent protein kinase-1	Y15748_at	100	-2,87
Nptx1	neuronal pentraxin 1	rc_AI072943_at	100	-2,82
Nrxn3	neurexin 3	L14851_at	100	-2,76
Chgb	chromogranin B	AF019974_at	100	-2,73
Ttr	transthyretin	rc_AA945169_g_at	100	-2,73
Cnr1	cannabinoid receptor 1 (brain)	X55812complete_seq_at	100	-2,67
Neurod1	neurogenic differentiation 1	D82074_at	100	-2,64
Mapt	microtubule-associated protein tau	rc_AA957930_s_at	100	-2,64
Atp2b2	ATPase, Ca++ transporting, plasma membrane 2	J03754Complete_seq_at	100	-2,6
Gpr51	G protein-coupled receptor 51	AF058795_at	100	-2,55
Mtap2	microtubule-associated protein 2	U30938_at	100	-2,52
Grm4	glutamate receptor, metabotropic 4	M90518_at	100	-2,49
Rtn1	reticulon 1	U17604_at	100	-2,46
Homer1	homer homolog 1 (Drosophila)	AF093268_s_at	100	-2,45
Cplx2	complexin 2	U35099_at	100	-2,45
Ptprd	protein tyrosine phosphatase, receptor type, D	L19180_g_at	100	-2,37
Neurod1	neurogenic differentiation 1	D82074_g_at	100	-2,36
Il6st	interleukin 6 signal transducer	M92340_at	100	-2,34
Plp	proteolipid protein	rc_AI072770_s_at	100	-2,34
Tm4sf3	transmembrane 4 superfamily member 3	Y13275_at	100	-2,34
Ptprd	protein tyrosine phosphatase, receptor type, D	L19933_s_at	100	-2,33
Kcnc3	potassium voltage gated channel member 3	rc_AI639023_at	100	-2,33
Ca2	carbonic anhydrase 2	X58294_at	100	-2,33
Ptpn5	protein tyrosine phosphatase, non-receptor type 5	S49400_at	100	-2,32
Cx3cl1	chemokine (C-X3-C motif) ligand 1	AF030358_g_at	100	-2,3
Gnao	guanine nucleotide binding protein, alpha o	M17526_g_at	100	-2,3
Sparc	secreted acidic cysteine rich glycoprotein	rc_AA891204_s_at	100	-2,27
Dnm1	dynamin 1	X54531mRNA_at	100	-2,24
Reln	reelin	rc_AA893471_s_at	100	-2,23
Agrn	agrin	M64780_g_at	100	-2,22
Hspa1a	heat shock 70kD protein 1A	Z75029_s_at	100	-2,21
Gria2	glutamate receptor, ionotropic, 2	M38061_at	100	-2,2
Ca2	carbonic anhydrase 2	U60578cds_s_at	100	-2,17
Nfia	nuclear factor I/A	X84210complete_seq_s_at	100	-2,16
Atp1a2	ATPase, Na+K+ transporting, alpha 2	rc_AI177026_at	100	-2,14
Rtn1	reticulon 1	X52817cds_s_at	100	-2,13
Lamp2	lysosomal membrane glycoprotein 2	M32016_at	100	-2,1
Tyro3	TYRO3 protein tyrosine kinase 3	D37880_at	100	-2,09
Camk2b	calcium/calmodulin-dependent protein kinase II beta sub.	M16112_g_at	100	-2,08
Pmp22	peripheral myelin protein 22	S55427_s_at	100	-2,08
Syt4	synaptotagmin 4	U14398_g_at	100	-2,08
Ler3	immediate early response 3	X96437mRNA_g_at	100	-2,07
Cpe	carboxypeptidase E	L07281_at	100	-2,06
Gtf2ird1	general transcription factor II I repeat domain-containing 1	rc_AA800912_g_at	100	-2,05
Rhob	rhoB gene	rc_AA900505_at	100	-2,04
Atp2a2	ATPase, Ca++ transporting, cardiac muscle, slow twitch 2	AA799276_at	100	-2,03
Rbs11	Rbs11 protein	U04808_at	100	-2,02
Sparcl1	SPARC-like 1 (mast9, hevin)	U27562_at	100	-2,02
Atp1b1	ATPase, Na+/K+ transporting, beta 1 polypeptide	rc_AI230614_s_at	100	-2,01
Slc16a7	solute carrier family 16, monocarboxylic acid transporters 7	U62316_at	100	-2,01

Table S4. Genes with increased expression in lymph node derived CD4+ cells of LEW.1AV1 (RT1^{av1}) rats. Two gene array chips with material derived from MOG 91-108-immunized rats were compared to chip data of material derived from MOG 73-90-immunized rats. The number of comparisons in which a given gene had a SLR above 1 were counted. If a gene had a SLR above 1 in 100% of the comparisons it was included in the analysis. ESTs, sequences not corresponding to a gene and duplicates were removed from the analysis. CNS-infiltrating cells were prepared as described (Weissert et al., 2001).

Gene Symbol	Gene Title	Affymetrix Probe set ID	CD4 MOG 91-108 vs MOG73-90 percentage	CD4 MOG 91-108 vs MOG73-90 average SLR
---	transcribed sequence with strong similarity to protein c-fos	1375043_at	100	6.02
Jun	v-jun sarcoma virus 17 oncogene homolog (avian)	1389528_s_at	100	4.61
Rgs2	regulator of G-protein signaling protein 2	1368144_at	100	4.01
Ptpn16	protein tyrosine phosphatase, non-receptor type 16	1368146_at	100	3.80
Ppp3r1	protein phospatase 3, reg. Sub. B, alpha isoform 1	1369152_at	100	3.41
Junb	Jun-B oncogene	1387788_at	100	3.22
Rgs2	regulator of G-protein signaling protein 2	1387074_at	100	3.21
RT1Aw2	RT1 class Ib gene(Aw2)	1370429_at	100	3.08
Copeb	core promoter element binding protein	1387060_at	100	2.58
Arhb	rhoB gene	1369958_at	100	2.29
Cd152	CD152 antigen	1387638_a_at	100	2.22
Rgc32	Rgc32 protein	1368080_at	100	2.07
Cxcr4	Chemokine receptor (LCR1)	1370097_a_at	100	2.04
Myd116	myeloid differentiation primary response gene 116	1370174_at	100	1.83
Znf22	zinc finger protein 22 (KOX 15)	1374780_at	100	1.75
Cmkbr4	chemokine (C-C) receptor 4	1369555_at	100	1.73
Cpg21	MAP-kinase phosphatase (cpg21)	1368124_at	100	1.69
Klf4	Kruppel-like factor 4 (gut)	1387260_at	100	1.67
Mafg	v-maf musculoaponeurotic fibrosarcoma (avian) onco. fam., prot.G	1368874_a_at	100	1.59
Snf1lk	SNF1-like kinase	1368596_at	100	1.40
Gadd45a	growth arrest and DNA-damage-inducible 45 alpha	1368947_at	100	1.36
Tob1	transducer of ERBB2, 1	1368132_at	100	1.34
Zfp36	zinc finger protein 36	1387870_at	100	1.21
Bhlhb2	basic helix-loop-helix domain containing, class B2	1369415_at	100	1.19
Nr4a1	immediate early gene transcription factor NGFI-B	1386935_at	100	1.17
LOC84349	CD40 ligand	1368800_at	100	1.16

Table S5. Genes with decreased expression in the CD4+ cells in the lymphnodes of LEW.1AV1 (RT1^{av1}) rats. The analysis was performed as described in Table S4.

Gene Symbol	Gene Title	Affymetrix Probe set ID	CD4 MOG 91-108 vs MOG73-90 percentage	CD4 MOG 91-108 vs MOG73-90 average SLR
RT1Aw2	RT1 class Ib gene(Aw2)	1370428_x_at	100	-5.82
Igb	immunoglobulin-associated beta	1387749_at	100	-3.74
Fcgr2	low affinity IG gamma FC region receptor II precursor	1371079_at	100	-3.25
Clu	clusterin	1367784_a_at	100	-3.03
Csn10	casein kappa	1369591_at	100	-2.71
Col3a1	collagen, type III, alpha 1	1370959_at	100	-2.70
Csn1	Casein, alpha	1388183_at	100	-2.66
RT1Aw2	RT1 class Ib gene(Aw2)	1370463_x_at	100	-2.59
Sh3bp5	SH3-domain binding protein 5 (BTK-associated)	1387294_at	100	-2.51
Lalba	lactalbumin, alpha	1387838_at	100	-2.30
Cd74	CD74 antigen	1367679_at	100	-2.19
Rtp801	HIF-1 responsive RTP801	1368025_at	100	-2.00
Hla-dmb	major histocompatibility complex, class II, DM beta	1370882_at	100	-1.97
Ctsh	cathepsin H	1386899_at	100	-1.94
Hla-dma	major histocompatibility complex, class II, DM alpha	1370904_at	100	-1.88
Igfbp5	insulin-like growth factor-binding protein 5	1370960_at	100	-1.86
Fn1	fibronectin 1	1370234_at	100	-1.81
Ccl5	chemokine (C-C motif) ligand 5	1369983_at	100	-1.79
Ptpns1	protein tyrosine phosphatase, non-r. type substrate 1	1367881_at	100	-1.70
Ogt	O linked N-acetylglucosamine transferase	1388758_at	100	-1.63
Pht2	peptide/histidine transporter PHT2	1370516_at	100	-1.58
Syk	spleen tyrosine kinase	1368186_a_at	100	-1.56
Enpep	aminopeptidase A	1371485_at	100	-1.48
Pkib	protein kinase (cAMP dependent, catalytic) inhibitor beta	1369105_a_at	100	-1.46
Lnk	linker of T-cell receptor pathways	1367723_a_at	100	-1.42
1C7	NK receptor 1c7	1378285_at	100	-1.42
Stx7	syntaxin 7	1387857_at	100	-1.42
Gpnmb	glycoprotein (transmembrane) nmb	1368187_at	100	-1.39
Abp10	annexin V-binding protein ABP-10	1389441_at	100	-1.36
Pxk	PX serine/threonine kinase	1390422_at	100	-1.34
Vamp1	vesicle-associated membrane protein 1	1373510_at	100	-1.33
Enpp2	ectonucleotide pyrophosphatase/phosphodiesterase 2	1368536_at	100	-1.32
Psmb8	proteosome (prosome, macropain) subunit, beta type 8	1367786_at	100	-1.29
RT1Aw2	RT1 class Ib gene(Aw2)	1389734_x_at	100	-1.28
Myr2	unconventional myosin Myr2 I heavy chain	1369631_at	100	-1.27
Scd2	stearoyl-Coenzyme A desaturase 2	1367668_a_at	100	-1.26
RT1.S3	MHC class Ib RT1.S3	1388213_a_at	100	-1.26
Cybb	endothelial type gp91-phox gene	1369181_at	100	-1.22
Atp2b1	ATPase, Ca++ transporting, plasma membrane 1	1370050_at	100	-1.21
Ppp3ca	protein phosphatase 3, catalytic subunit, alpha isoform	1368277_at	100	-1.19
Igf2r	insulin-like growth factor 2 receptor	1386872_at	100	-1.15
Clasp2	CLIP-associating protein 2	1368099_at	100	-1.14
Ppp3ca	protein phosphatase 3, catalytic subunit, alpha isoform	1373479_at	100	-1.14
Mca32	surface protein MCA-32	1368610_at	100	-1.13
Slc7a7	solute carrier family 7	1387808_at	100	-1.12
Crot	carnitine O-octanoyltransferase	1368426_at	100	-1.09
Cltc	clathrin, heavy polypeptide (Hc)	1398842_at	100	-1.09

Table S6. Group characteristics of patients with RRMS and SPMS as well as controls.

RRMS, relapsing remitting MS; SPMS, secondary progressive MS.

Group	*CXCR4* mRNA expression				CXCL12 protein			
	Age [mean]	Number, male/female [n]	EDSS [mean)	EDSS [range, median]	Age [mean]	Number, male/female [n]	EDSS [mean)	EDSS [range, median)
Control	39	25, 10/15	0	0, 0	36	21, 7/14	0	0, 0
RRMS	36	32, 8/24	1.2	0-4, 1	36	24, 7/17	1.6	0-4, 1
SPMS	46	22, 7/15	5.1	2-7, 5	45	28, 9/19	5.3	2-7, 5

Table S7. Characteristics of MS patients and controls. RRMS, relapsing remitting MS; SPMS, secondary progressive MS. BRAC, Betaferon, Rebif, Avonex, Copaxone. EDSS, expanded disability status scale.

Person	Gender	Age	Type	Immunomodulatory treatment	EDSS	Sample used for	
						CXCR4 mRNA	CXCL12
1	Male	67	Control			X	
2	Female	32	Control			X	
3	Male	28	Control			X	X
4	Female	27	Control			X	
5	Female	60	Control			X	
6	Female	32	Control			X	
7	Female	24	Control			X	X
8	Male	67	Control			X	
9	Male	27	Control			X	
10	Male	24	Control			X	X
11	Female	22	Control			X	X
12	Male	29	Control			X	X
13	Female	27	Control			X	X
14	Female	39	Control			X	X
15	Male	23	Control			X	X
16	Male	25	Control			X	X
17	Female	58	Control			X	X
18	Female	56	Control			X	X
19	Female	60	Control			X	X
20	Female	41	Control			X	X
21	Male	39	Control			X	X
22	Male	67	Control			X	X
23	Female	30	Control			X	X
24	Female	38	Control			X	X
25	Female	26	Control			X	X
26	Female	27	Control				X
27	Female	30	Control				X
28	Female	37	Control				X
29	Female	35	RRMS	BRAC	1	X	X
30	Male	36	RRMS	None	2	X	X
31	Female	45	RRMS	None	3.5	X	X
32	Female	34	RRMS	BRAC	0	X	X
33	Female	36	RRMS	None	0	X	X
34	Female	38	RRMS	BRAC	4	X	X
35	Female	41	RRMS	None	2	X	
36	Female	34	RRMS	None	2	X	X
37	Female	27	RRMS	None	1	X	
38	Male	37	RRMS	None	1	X	X
39	Female	23	RRMS	None	1	X	X
40	Female	23	RRMS	None	2.5	X	X
41	Male	32	RRMS	BRAC	1	X	X
42	Male	40	RRMS	BRAC	3	X	X
43	Female	37	RRMS	None	1.5	X	X
44	Female	38	RRMS	BRAC	0	X	
45	Female	53	RRMS	BRAC	3.5	X	X
46	Female	37	RRMS	None	0	X	X
47	Male	33	RRMS	BRAC	0	X	
48	Female	32	RRMS	None	1	X	
49	Male	36	RRMS	BRAC	1.5	X	X
50	Female	30	RRMS	BRAC	0	X	X
51	Female	35	RRMS	BRAC	0	X	X
52	Female	51	RRMS	BRAC	1.5	X	X
53	Female	36	RRMS	BRAC	1	X	X
54	Male	38	RRMS	None	1	X	X
55	Female	42	RRMS	None	0	X	X
56	Female	37	RRMS	BRAC	1.5	X	
57	Female	31	RRMS	None	2	X	
58	Female	37	RRMS	None	1	X	
59	Female	35	RRMS	BRAC	0	X	X
60	Male	27	RRMS	None	2	X	X
61	Female	63	SPMS	None	5	X	X
62	Male	58	SPMS	None	6	X	X
63	Female	51	SPMS	None	6	X	X
64	Male	43	SPMS	None	3.5	X	X
65	Female	48	SPMS	None	3.5	X	X
66	Female	37	SPMS	BRAC	5	X	X
67	Male	32	SPMS	None	7	X	X
68	Female	64	SPMS	None	6.5	X	X
69	Female	43	SPMS	None	6	X	X
70	Female	34	SPMS	None	4	X	X
71	Male	58	SPMS	None	5	X	
72	Female	42	SPMS	None	4	X	X
73	Female	31	SPMS	None	4	X	X
74	Male	37	SPMS	BRAC	5.5	X	X
75	Female	38	SPMS	None	4	X	X
76	Female	41	SPMS	Mitoxantrone	6.5	X	X
77	Female	36	SPMS	None	5	X	X
78	Male	65	SPMS	None	6.5	X	X
79	Female	51	SPMS	None	5	X	X
80	Male	41	SPMS	None	2.5		X
81	Female	48	SPMS	BRAC	6	X	X
82	Female	39	SPMS	BRAC	2.5		X
83	Male	42	SPMS	BRAC	6	X	X
84	Female	42	SPMS	None	2	X	X
85	Male	60	SPMS	None	6		X
86	Male	40	SPMS	BRAC	5.5		X
87	Female	52	SPMS	None	4		X
88	Female	43	SPMS	None	5		X
89	Female	56	SPMS	None	4		X

Fig. S1. Representative FACS dot blot analysis of cells from draining lymph nodes of a FTY720 treated DA (RT1^{av1}) rat (rat no. 3187) compared to a vehicle treated control (rat no. 3189). Data analysis was performed with Flowing Software 2.5.1 (Turku Center for Biotechnology).

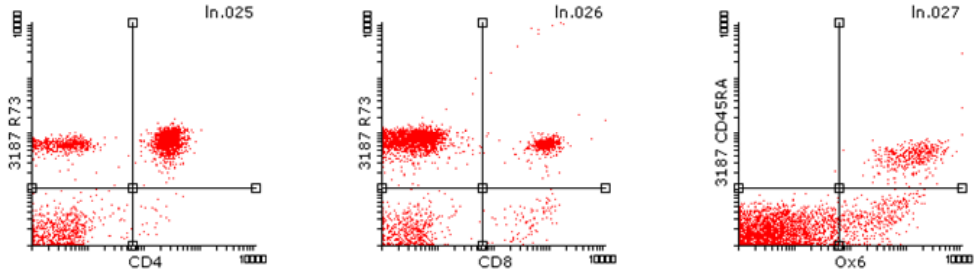

FTY720 treatment

	All events: Events	All events: % of Vis	Left Bottom: % of Vis	Right Bottom: % of Vis	Left Top: % of Vis	Right Top: % of Vis
In.025	3.602	100,00	17,74	0,56	15,96	65,74
In.026	3.692	100,00	14,95	2,44	66,82	15,79
In.027	3.438	100,00	77,05	10,82	0,03	12,10

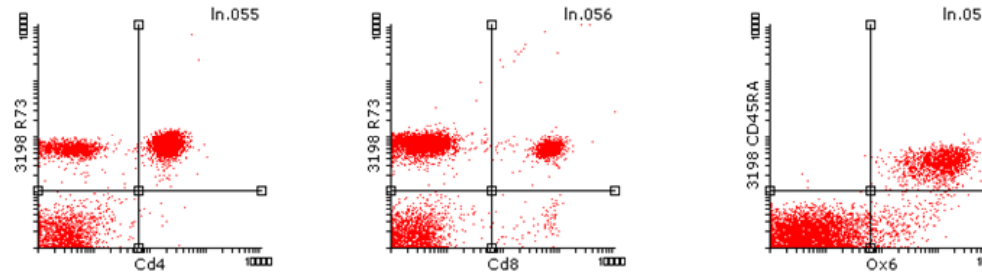

Vehicle Control

	All events: Events	All events: % of Vis	Left Bottom: % of Vis	Right Bottom: % of Vis	Left Top: % of Vis	Right Top: % of Vis
In.055	6.437	100,00	24,65	0,20	20,12	55,03
In.056	6.405	100,00	26,00	1,25	52,96	19,80
In.057	6.515	100,00	71,74	4,57	0,06	23,62